

Nonequilibrium occupation number and charge susceptibility of a resonance level close to a dissipative quantum phase transition

Chung-Hou Chung^{1,2}, K.V.P. Latha^{1,3}

¹*Electrophysics Department, National Chiao-Tung University, HsinChu, Taiwan R.O.C. 300*

²*Departments of Physics and Applied Physics, Yale University, New Haven, CT, 06511 USA*

³*Institute of applied physics, Academia Sinica, NanKang, Taipei, Taiwan R.O.C. 11529*

(Dated: May 6, 2021)

Based on the recent paper (Phys. Rev. Lett. **102**, 216803, (2009)), we study the nonequilibrium occupation number n_d and charge susceptibility χ of a resonance level close to dissipative quantum phase transition of the Kosterlitz-Thouless (KT) type between a de-localized phase for weak dissipation and a localized phase for strong dissipation. The resonance level is coupled to two spinless fermionic baths with a finite bias voltage and an Ohmic bosonic bath representing the dissipative environment. The system is equivalent to an effective anisotropic Kondo model out of equilibrium. Within the nonequilibrium Renormalization Group (RG) approach, we calculate nonequilibrium magnetization M and spin susceptibility χ in the effective Kondo model, corresponding to $2n_d - 1$ and χ of a resonance level, respectively. We demonstrate the smearing of the KT transition in the nonequilibrium magnetization M as a function of the effective anisotropic Kondo couplings, in contrast to a perfect jump in M at the transition in equilibrium. In the limit of large bias voltages, we find M and χ at the KT transition and in the localized phase show deviations from the equilibrium Curie-law behavior. As the system gets deeper in the localized phase, both $n_d - 1/2$ and χ decrease more rapidly to zero with increasing bias voltages.

PACS numbers: 72.15.Qm, 7.23.-b, 03.65.Yz

Introduction

Quantum phase transitions (QPTs)[1, 2] due to competing quantum ground states in strongly correlated systems have been extensively investigated over the past decades. Near the transitions, exotic quantum critical properties are realized. In recent years, there has been a growing interest in QPTs in nanosystems[3–8]. Very recently, QPTs have been extended to nonequilibrium nanosystems where little is known regarding nonequilibrium transport near the transitions. A generic example[11] is the transport through a dissipative resonance-level (spinless quantum dot) at a finite bias voltage where dissipative bosonic bath (noise) coming from the environment in the leads gives rise to quantum phase transition in transport between a conducting (de-localized) phase where resonant tunneling dominates and an insulating (localized) phase where the dissipation prevails. In fact, dissipative quantum phase transitions have been investigated in various systems[9, 10]. Nevertheless, much of the attention has been focused on equilibrium properties; while very little is known on the nonequilibrium properties. The bias voltage V plays a very different role as the temperature T in equilibrium systems as the voltage-induced decoherence behaves very differently from the decoherence at finite temperature, leading to exotic transport properties near the quantum phase transition compared to that in equilibrium at finite temperatures.

Based on the recent work in Ref. [11] on nonequilibrium transport of a dissipative resonance-level at the

Kosterlitz-Thouless (KT) type de-localized-to-localized quantum transition, we study in this paper the nonequilibrium occupation number and charge susceptibility of a resonance-level quantum dot subjected to a noisy environment near the phase transition. In equilibrium, it has been shown that the occupation number $n(\epsilon)$ of a dissipative resonance-level shows a jump at the Fermi energy at the KT transition and in the localized phase where ϵ is an infinitesimal shift in the energy of the resonance-level[3, 6]. At finite temperatures and in equilibrium, a crossover in $n_d(\epsilon)$ replaces the jump and in the high temperature limit it is determined by the thermal magnetization of a free spin; hence the Curie law behavior is expected. On the other hand, when a large bias voltage is applied on the system at $T = 0$, however, very little is known about the nonequilibrium effects on the occupation number and charge susceptibility. By first mapping our system onto an effective Kondo model and applying the recently developed frequency-dependent Renormalization Group (RG) approach[12] to the nonequilibrium Kondo effect of a quantum dot, we calculate the occupation number and charge susceptibility of a resonance-level near the transition. Near the transition, we find distinct nonequilibrium behaviors of these quantities from those in equilibrium.

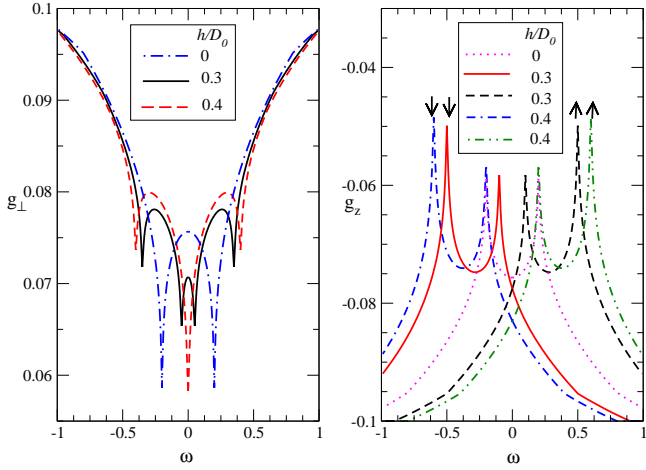


FIG. 1: (Color online) $g_{\perp,z}(\omega)$ versus ω at the KT transition. (a). $g_{\perp}(\omega)$. (b). $g_{z\sigma}(\omega)$. Arrows indicate spin σ of the corresponding curve. The bare couplings are $g_{\perp} = -g_z = 0.1D_0$; bias voltage is fixed at $V = 0.4D_0$; the effective magnetic fields are fixed at $h = 0, 0.3D_0, 0.4D_0$. Here, $D_0 = 1$ for all the figures.

Model Hamiltonian

The starting point is a spin-polarized quantum dot coupled to two Fermi-liquid leads subjected to noisy Ohmic environment, which coupled capacitively to the quantum dot. The noisy environment here consists of a collection of harmonic oscillators with the Ohmic correlation: $G_{\phi}(i\omega) \equiv \langle \phi(i\omega)\phi(-i\omega) \rangle = 2\pi \frac{R}{R_k} [|\omega| + \frac{\omega^2}{\omega_c}]^{-1}$ with R being the circuit resistance and $R_k \equiv 2\pi\hbar/e^2 \approx 25.8k\Omega$ being the quantum resistance. For a dissipative resonant level (spinless quantum dot) model, the quantum phase transition separating the conducting and insulating phase for the level is solely driven by dissipation. Our Hamiltonian is given by:

$$\begin{aligned}
H = & \sum_{k,i=1,2} (\epsilon(k) - \mu_i) c_{ki}^{\dagger} c_{ki} + t_i c_{ki}^{\dagger} d + h.c. \\
& + \sum_r \lambda_r (d^{\dagger} d - 1/2) (b_r + b_r^{\dagger}) + \sum_r \omega_r b_r^{\dagger} b_r, \\
& + h(d^{\dagger} d - 1/2)
\end{aligned} \quad (1)$$

where t_i is the hopping amplitude between the lead i and the quantum dot, c_{ki} and d are electron operators for the Fermi-liquid leads and the quantum dot, respectively, $\mu_i = \pm V/2$ is the chemical potential (bias voltage) applied on the lead i , while h is the energy level of the dot. We assume that the electron spins have been polarized by a strong magnetic field. Here, b_{α} are the boson operators of the dissipative bath with an ohmic spectral density [4]: $J(\omega) = \sum_r \lambda_r^2 \delta(\omega - \omega_r) = \alpha\omega$ with α being the strength of the dissipative boson bath.

First, through similar bosonization and refermionization procedures as in equilibrium [3–6], we map our model to

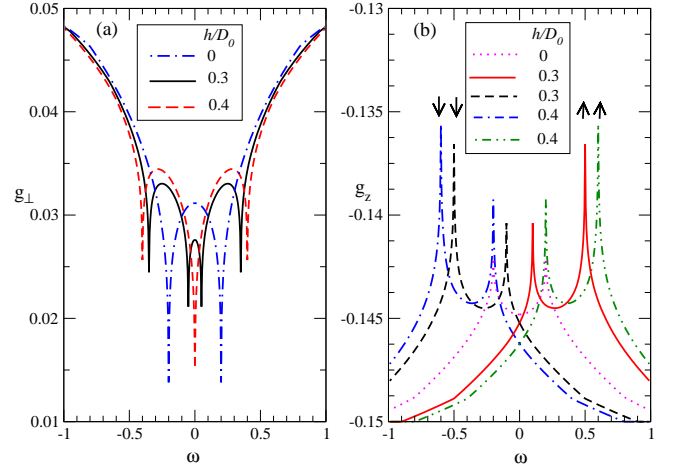


FIG. 2: (Color online) $g_{\perp,z}(\omega)$ versus ω in the localized phase. (a). $g_{\perp}(\omega)$. (b). $g_{z\sigma}(\omega)$. Arrows indicate spin σ of the corresponding curve. The bare couplings are $g_{\perp} = 0.05D_0$, $g_z = -0.15D_0$; bias voltage is fixed at $V = 0.4D_0$; the effective magnetic fields are fixed at $h = 0, 0.3D_0, 0.4D_0$. Here, $D_0 = 1$ for all the figures.

an equivalent anisotropic Kondo model in an effective magnetic field h with the effective left L and right R Fermi-liquid leads[11]. The effective Kondo model takes the form:

$$\begin{aligned}
H_K = & \sum_{k,\gamma=L,R,\sigma=\uparrow,\downarrow} [\epsilon_k - \mu_{\gamma}] c_{k\gamma\sigma}^{\dagger} c_{k\gamma\sigma} \\
& + (J_{\perp}^1 s_{LR}^+ S^- + J_{\perp}^2 s_{RL}^+ S^- + h.c.) \\
& + \sum_{\gamma=L,R} J_z s_{\gamma\gamma}^z S^z + h S_z,
\end{aligned} \quad (2)$$

where $c_{kL(R)\sigma}^{\dagger}$ is the electron operator of the effective lead $L(R)$, with spin σ . Here, the spin operators are related to the electron operators on the dot by: $S^+ = d^{\dagger}$, $S^- = d$, and $S^z = d^{\dagger} d - 1/2 = n_d - 1/2$ where $n_d = d^{\dagger} d$ describes the charge occupancy of the level. The spin operators for electrons in the effective leads are $s_{\gamma\beta}^{\pm} = \sum_{\alpha,\delta,k,k'} 1/2 c_{k\gamma\alpha}^{\dagger} \sigma_{\alpha\delta}^{\pm} c_{k'\beta\delta}$, the transverse and longitudinal Kondo couplings are given by $J_{\perp}^{1(2)} \propto t_{1(2)}$ and $J_z \propto 1/2(1 - 1/\sqrt{2\alpha^*})$ respectively, and the effective bias voltage is $\mu_{\gamma} = \pm \frac{V}{2} \sqrt{1/(2\alpha^*)}$, where $1/\alpha^* = 1 + \alpha$. Note that $\mu_{\gamma} \rightarrow \pm V/2$ near the transition ($\alpha^* \rightarrow 1/2$ or $\alpha \rightarrow 1$) where the above mapping is exact. The spin operator of the quantum dot in the effective Kondo model \vec{S} can also be expressed in terms of spinful pseudofermion operator f_{σ} : $S_{i=x,y,z} = f_{\alpha}^{\dagger} \sigma_{i=x,y,z}^{\alpha\beta} f_{\beta}$. In the Kondo limit where only the singly occupied fermion states are physically relevant, a projection onto the singly occupied states is necessary in the pseudofermion representation, which can be achieved by introducing the Lagrange multiplier λ so that $Q = \sum_{\gamma} f_{\gamma}^{\dagger} f_{\gamma} = 1$. An observable \mathcal{A} is defined as[12]:

$$\langle \mathcal{A} \rangle_{Q=1} = \lim_{\lambda \rightarrow \infty} \frac{\langle \mathcal{A} Q \rangle_{\lambda}}{\langle Q \rangle_{\lambda}} \quad (3)$$

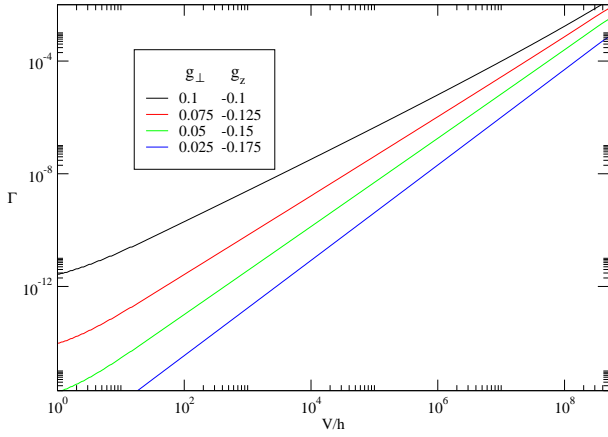


FIG. 3: (Color online) Γ versus V/h for different bare Kondo couplings. Here, the bare Kondo couplings $g_{\perp,z}$ are in units of D_0 , and $h = 10^{-9}D_0$ with $D_0 = 1$.

In equilibrium, the above anisotropic Kondo model exhibits the Kosterlitz-Thouless transition from a de-localized phase with a finite conductance $G \approx \frac{1}{2\pi\hbar}$ ($e = \hbar = 1$) for $J_{\perp} + J_z > 0$ to a localized phase for $J_{\perp} + J_z \leq 0$ with vanishing conductance. The nonequilibrium transport near the KT transition exhibits distinct profile from that in equilibrium and it has been addressed in Ref. [11]. We will focus here on the nonequilibrium occupation number and charge susceptibility near the KT transition. At the KT transition ($J_{\perp} = -J_z$) and in the localized phase, we expect in equilibrium a perfect jump in $\langle n_d \rangle$ (or $\langle S_z \rangle$): $\langle n_d \rangle = 1$ for $h > 0$ and $\langle n_d \rangle = 0$ for $h < 0$ [3]. At a finite bias voltage, however, instead of a jump we expect $\langle n_d \rangle$ shows a smooth crossover as a function of h/V .

Nonequilibrium RG formalism

The non-equilibrium perturbative renormalization group (RG) equations for the effective Kondo model in a magnetic field are obtained by considering the generalized frequency dependent Kondo couplings in the Keldysh formulation followed Ref. [12]:

$$\begin{aligned} \frac{\partial g_{\sigma,z}(\omega)}{\partial \ln D} &= -\frac{1}{2} \sum_{\sigma\beta=-1,1} \left[g_{\sigma\perp} \left(\frac{\beta V + \sigma h}{2} \right) \right]^2 \Theta_{\omega+\sigma[h+\frac{\beta V}{2}]} \\ \frac{\partial g_{\sigma,\perp}(\omega)}{\partial \ln D} &= -\frac{1}{2} \sum_{\sigma\beta=-1,1} g_{\sigma,\perp} \left(\frac{\beta V + \sigma h}{2} \right) \times \\ &g_{\sigma,z} \left(\frac{\beta V + \sigma h}{2} \right) \Theta_{\omega+\frac{\beta V+\sigma h}{2}}, \end{aligned} \quad (4)$$

where $g_{\perp\sigma}(\omega) = N(0)J_{\perp\sigma}^1 = N(0)J_{\perp\sigma}^2$, $g_{z\sigma}(\omega) = N(0)J_{z\sigma}$ are dimensionless frequency-dependent Kondo

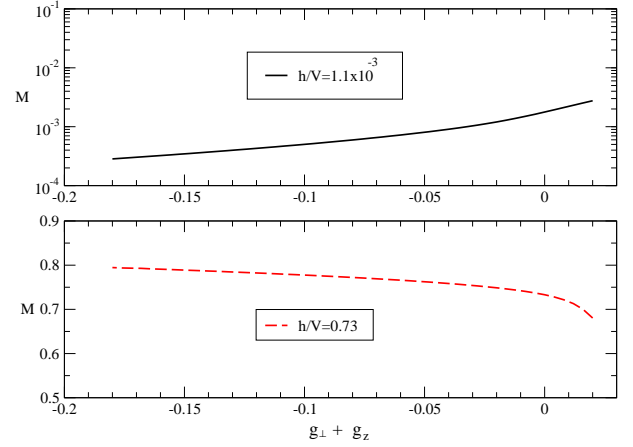


FIG. 4: (Color online) Nonequilibrium magnetization M in the effective Kondo model at fixed $h \approx 9.6 \times 10^{-8}D_0$ and fixed bias voltage V (small bias with $h/V \approx 0.73$ for lower pannel and large bias with $h/V \approx 1.1 \times 10^{-3}$ for upper panel) versus the initial (bare) Kondo couplings $g_{\perp} + g_z$ across the KT transition between the delocalized phase ($g_{\perp} + g_z > 0$) and the localized phase ($g_{\perp} + g_z < 0$). Here, the bare Kondo couplings $g_{\perp,z}$ are in units of D_0 with $D_0 = 1$.

couplings with $N(0)$ being density of states per spin of the conduction electrons (we assume symmetric hopping $t_1 = t_2 = t$), $\Theta_{\omega} = \Theta(D - |\omega + i\Gamma|)$, $D < D_0$ is the running cutoff, and Γ is the decoherence (dephasing) rate at finite bias which cuts off the RG flow [12], given by

$$\begin{aligned} \Gamma &= \sum_{\sigma} \frac{\pi}{4\hbar} \int d\omega f_{\omega}^L (1 - f_{\omega}^L) [g_{\sigma,z}(\omega)]^2 + \\ &f_{\omega-\sigma h/2}^L (1 - f_{\omega+\sigma h/2}^R) [g_{\perp}(\omega)]^2 + (L \rightarrow R) \end{aligned} \quad (5)$$

where f_{ω} is the Fermi function given by $f(\omega) = 1/(1 + e^{\omega/kT})$. Note that the Kondo couplings exhibit the following symmetries: $g_{\sigma,\perp}(\omega) = g_{-\sigma,\perp}(\omega) = g_{\sigma,\perp}(-\omega) \equiv g_{\perp}(\omega)$, $g_{\sigma,z}(\omega) = g_{-\sigma,z}(-\omega)$. We have solved the RG equations subject to Eq. 5 self-consistently. The solutions for $g_{\perp}(\omega)$ and $g_{\sigma,z}(\omega)$ at the transition are shown in Fig. 1. Similar behaviors for $g_{z\sigma,\perp}(\omega)$ are obtained in the localized phase. The decoherence rate $\Gamma(V/h)$ is plotted in Fig. 3.

Note that, unlike the equilibrium RG at finite temperatures where RG flows are cutoff by temperature T , here in nonequilibrium the RG flows will be cutoff by the decoherence rate Γ , a much lower energy scale than V , $\Gamma \ll V$. This explains the dips (peaks) structure in $g_{\perp(z)}(\omega)$ in Fig. 1 and Fig. 2. In contrast, the equilibrium RG will lead to approximately frequency independent couplings, (or ‘‘flat’’ functions $g_{\perp}(\omega) \approx g_{\perp,z}(\omega = 0)$). In the absence of field $h = 0$, $g_{\perp(z)}(\omega)$ show dips (peaks) at $\omega = \pm V/2$. In the presence of both bias V and field h , $g_{\perp}(\omega)$ shows dips at $\omega = \pm \frac{V+h}{2}$; while $g_{z\uparrow(\downarrow)}$ show peaks at $\omega = h \pm V/2$

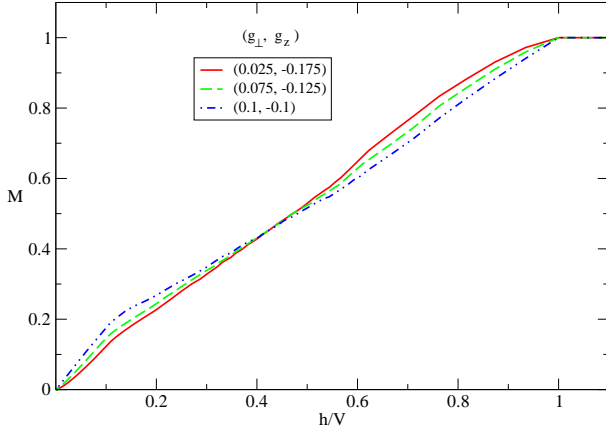


FIG. 5: (Color online) Nonequilibrium magnetization $M(h/V)$ in the effective Kondo model at the KT transition and in the localized phase. Here, the bare Kondo couplings $g_{\perp,z}$ are in units of D_0 , and $h = 10^{-9}D_0$ with $D_0 = 1$.

($\omega = -h \pm V/2$)[12]. At $h = V$, two dips of $g_{\perp}(\omega)$ at $\omega = \frac{V-h}{2}$ and $\omega = \frac{-V+h}{2}$ merge into a large dip at $\omega = 0$. We use the solutions of the frequency-dependent Kondo couplings $g_{\perp,z\sigma}(\omega)$ to compute the occupation number and charge susceptibility of the resonance-level near the transition.

Occupation number and magnetization

From the mapping, the occupation number of the resonance level $n_d = d^\dagger d$ is related to the magnetization of the pseudofermion in the effective Kondo model by $S_z = n_d - 1/2 = \frac{M}{2}$ where $M = n_{\uparrow} - n_{\downarrow} = f_{\uparrow}^{\dagger} f_{\uparrow} - f_{\downarrow}^{\dagger} f_{\downarrow}$. Since the occupation number in the dissipative resonance-level is related to the pseudospin magnetization in the effective Kondo model by a simple linear relation, in the following we will use the properties of the magnetization M to represent those of the occupation number. The nonequilibrium occupation number of the pseudofermion $n_{\uparrow(\downarrow)} = f_{\uparrow(\downarrow)}^{\dagger} f_{\uparrow(\downarrow)}$ in the effective model can be determined by solving the Keldysh component of the Dyson equation for the pseudofermion self-energy[12], given by

$$n_{\alpha}(\omega) = (1 - \Sigma_{\alpha}^{>}(\omega)/\Sigma_{\alpha}^{<}(\omega))^{-1}, \quad (6)$$

Here, the nonequilibrium pseudofermion self-energies $\Sigma^{<(>)}(\omega)$ are obtained via renormalized perturbation theory up to second order in $g_{\gamma\gamma'}$:

$$\begin{aligned} \Sigma_{\alpha}^{<}(\omega) &= \sum_{\gamma,\gamma'=L,R} i[n_{\alpha}(-\frac{\alpha h}{2})\chi_{\gamma\gamma'}^{>,z}(-\omega - \frac{\alpha h}{2}) \\ &\quad + n_{-\alpha}(\frac{\alpha h}{2})\chi_{\gamma\gamma'}^{>,\perp}(-\omega + \frac{\alpha h}{2})], \\ \Sigma_{\alpha}^{>}(\omega) &= \sum_{\gamma,\gamma'=L,R} -i[\chi_{\gamma\gamma'}^{<,z}(-\omega - \frac{\alpha h}{2}) \end{aligned}$$

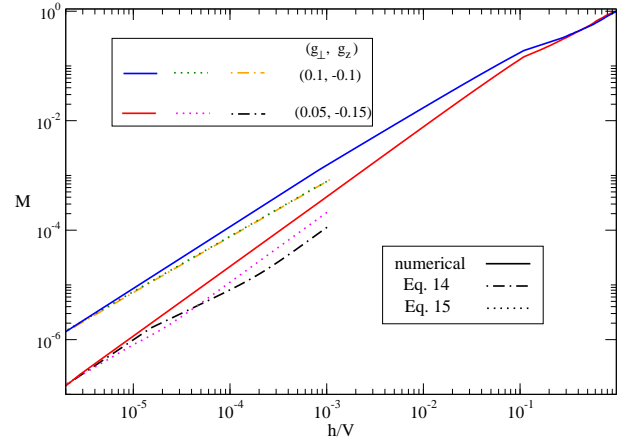


FIG. 6: (Color online) Nonequilibrium magnetization $M(h/V)$ in the effective Kondo model at the KT transition and in the localized phase. The dot-dash (dot) lines are results via Eq. 14 (15). Here, the bare Kondo couplings $g_{\perp,z}$ are in units of D_0 , and $h = 10^{-9}D_0$ with $D_0 = 1$.

$$+ \chi_{\gamma\gamma'}^{<,\perp}(-\omega + \frac{\alpha h}{2})] \quad (7)$$

where

$$\begin{aligned} \chi_{\gamma\gamma'}^{>,z}(\omega) &= \int d\epsilon [g_{\gamma\gamma'}^z(\epsilon)]^2 \delta_{\gamma\gamma'} f_{\gamma'}(\epsilon) [1 - f_{\gamma}(\epsilon + \omega)] \\ \chi_{\gamma\gamma'}^{>,\perp}(\omega) &= \int d\epsilon [g_{\gamma\gamma'}^{\perp}(\epsilon)]^2 \tau_{\gamma\gamma'}^{\perp} f_{\gamma'}(\epsilon) [1 - f_{\gamma}(\epsilon + \omega)] \end{aligned} \quad (8)$$

with τ^{\perp} being the x -component of the Pauli matrices. Similarly, $\chi_{\gamma\gamma'}^{<,z(\perp)}(\omega)$ are obtained by interchanging $f_{\gamma'}(\epsilon)$ and $[1 - f_{\gamma}(\epsilon + \omega)]$ in $\chi_{\gamma\gamma'}^{>,z(\perp)}(\omega)$. The nonequilibrium occupation number $n_{\uparrow}(\omega = -\frac{h}{2})$ is given by:

$$n_{\uparrow}(-\frac{h}{2}) = \frac{\sum_{\gamma\gamma'} \chi_{\gamma\gamma'}^{>,\perp}(h)}{\sum_{\gamma\gamma'} [\chi_{\gamma\gamma'}^{>,\perp}(h) + \chi_{\gamma\gamma'}^{<,\perp}(h)]} \quad (9)$$

The nonequilibrium magnetization M is therefore given by:

$$M = \frac{\sum_{\gamma\gamma'} [\chi_{\gamma\gamma'}^{>,\perp}(h) - \chi_{\gamma\gamma'}^{<,\perp}(h)]}{\sum_{\gamma\gamma'} [\chi_{\gamma\gamma'}^{>,\perp}(h) + \chi_{\gamma\gamma'}^{<,\perp}(h)]} \quad (10)$$

We can further simplify M as:

$$\begin{aligned} M &= \frac{A - B}{A + B}, \\ A &= \sum_{\alpha\alpha'=L,R} \int d\omega g_{\alpha\alpha'\perp}^2(\omega) f_{\omega-\mu_{\alpha}} (1 - f_{\omega-\mu_{\alpha'}-h}) \\ B &= \sum_{\alpha\alpha'=L,R} \int d\omega g_{\alpha\alpha'\perp}^2(\omega) f_{\omega-\mu_{\alpha}} (1 - f_{\omega-\mu_{\alpha'}+h}) \end{aligned} \quad (11)$$

At $T = 0$, magnetization M takes the following simple form:

$$M = \frac{\int_{\frac{V-h}{2}}^{\frac{V+h}{2}} d\omega g_{\perp}^2(\omega) + \int_{\frac{-V-h}{2}}^{\frac{-V+h}{2}} d\omega g_{\perp}^2(\omega)}{\int_{\frac{-V-h}{2}}^{\frac{V+h}{2}} d\omega g_{\perp}^2(\omega) + \int_{\frac{-V+h}{2}}^{\frac{V-h}{2}} d\omega g_{\perp}^2(\omega)} \quad (12)$$

Note that occupation number $n_{\uparrow(\downarrow)}$ can also be determined by the rate equation[12]: $\Gamma_{\uparrow\rightarrow\downarrow} = \Gamma_{\downarrow\rightarrow\uparrow}$ or $n_{\uparrow}\mathcal{A} = n_{\downarrow}\mathcal{B}$ where $\Gamma_{\downarrow\rightarrow\uparrow}$ is the spin-flip rate of pseudofermion from spin-down to spin-up state.

We have calculated the magnetization $M(h/V)$ numerically at the KT transition and in the localized phase for both small bias limit $V \approx h \ll D_0$ and large bias limit $V \gg h$ where we have fixed h at a small value. First, we demonstrate that the nonequilibrium magnetization M with a fixed $h \approx 9.6 \times 10^{-8} D_0$ for both fixed small (lower panel of Fig. 4) and large (upper panel of Fig. 4) bias voltages shows a smooth crossover as a function of $g_{\perp} + g_z$ across the KT transition ($g_{\perp} + g_z = 0$), in contrast to a perfect jump in M at the transition in equilibrium[3].

To investigate further the crossover behavior of the magnetization M , we calculate M as a function of h/V with h being fixed at a small value $h \approx 1.0 \times 10^{-9} D_0$. The result is shown in Fig. 5. First, let us examine simple limits from the numerical results. The spin of the quantum dot gets fully polarized $M = 1$ only when magnetic field h exceeds the bias voltage, $h \geq V$; while for $h < V$ the magnetization is reduced due to finite spin-flip decoherence rate. In the extreme large bias limit, $V \gg h$, we find M gets further suppression.

To gain more understanding of the numerical results, we obtain an analytic approximated form for $M(h/V)$ for $h \leq V$. For $V \rightarrow h$, $M \rightarrow 1$ in the following approximated form:

$$M \approx \frac{h}{(V-h) \frac{g_{\perp}^2(0)}{g_{\perp}^2(V/2)} + h}; \quad (13)$$

while in the large bias limit, $V/h \gg 1$, we find $M(h/V)$ has the following approximated form:

$$M \approx \frac{hg_{\perp}^2(V/2)}{(V-h) [\frac{\pi}{4}g_{\perp}^2(0) + (1-\frac{\pi}{4})g_{\perp}^2(\frac{V-h}{2})] + hg_{\perp}^2(V/2)} \quad (14)$$

Here, we have treated $g_{\perp}(\omega)^2$ within the interval $-\frac{V-h}{2} < \omega < \frac{V-h}{2}$ as a semi-ellipse. From Eq. 13 and Eq. 14, it is clear that the behaviors of the magnetization $M(h/V)$ depend sensitively on the dip-peak structure in $g_{\perp}(\omega)$, especially on the ratio $g_{\perp}(0)/g_{\perp}(V/2)$, and $g_{\perp}(\frac{V-h}{2})/g_{\perp}(V/2)$. In general, the analytical approximated forms for $g_{\perp}(\omega)$ at $\omega = 0, \frac{V}{2}, \frac{V-h}{2}$ are rather complex. Nevertheless, the values of $g_{\perp}(\omega)$ at these specific values of ω can be obtained numerically (see, for example Fig. 7).

In the extremely large bias limit, $h/V \rightarrow 0$, M is well

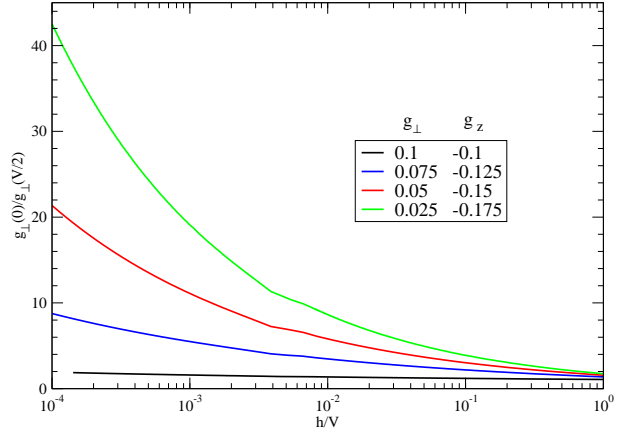


FIG. 7: (Color online) $g_{\perp}(\omega = 0)/g_{\perp}(\omega = V/2)$ versus h/V at the KT transition and in the localized phase. Here, the bare Kondo couplings $g_{\perp,z}$ are in units of D_0 , and $h = 10^{-9} D_0$ with $D_0 = 1$.

approximated by[11]

$$M \approx \frac{hg_{\perp}^2(V/2)}{V [\frac{\pi}{4}g_{\perp}^2(0) + (1-\frac{\pi}{4})g_{\perp}^2(\frac{V}{2})]} \quad (15)$$

In this limit, the explicit voltage dependence of $g_{\perp,cr}(\omega = 0, V/2)$ at the KT transition are given by[11]:

$$g_{\perp,cr}(\omega = 0) \approx \frac{1}{2 \ln(D/V)},$$

$$g_{\perp,cr}(\omega = V/2) \approx 1 / \ln\left(\frac{D^2}{\Gamma V}\right), \quad (16)$$

Similarly, $g_{\perp}(\omega = 0, V/2)_{loc}$ in the localized phase take the following forms:

$$g_{\perp,loc}(\omega = 0) - g_{\perp} \approx$$

$$\frac{A}{2c} \left[\left(\frac{V}{D_0}\right)^{2c} \sqrt{c^2 + A^2 \left(\frac{V}{D_0}\right)^{4c}} - \sqrt{A^2 + c^2} \right]$$

$$+ \frac{B}{c} \left[\left(\frac{V}{2D_0}\right)^c \sqrt{c^2 + B^2 \left(\frac{V}{2D_0}\right)^{2c}} \right.$$

$$\left. - \left(\frac{V}{D_0}\right)^c \sqrt{c^2 + B^2 \left(\frac{V}{D_0}\right)^{2c}} \right], \quad (17)$$

$$g_{\perp,loc}(\omega = V/2) - g_{\perp} \approx$$

$$\frac{A}{2c} \left[\left(\frac{V}{D_0}\right)^{2c} \sqrt{c^2 + A^2 \left(\frac{V}{D_0}\right)^{4c}} - \sqrt{A^2 + c^2} \right]$$

$$+ \frac{B}{2c} \left[\left(\frac{\Gamma}{D_0}\right)^c \sqrt{c^2 + B^2 \left(\frac{\Gamma}{D_0}\right)^{2c}} \right.$$

$$\left. - \left(\frac{V}{D_0}\right)^c \sqrt{c^2 + B^2 \left(\frac{V}{D_0}\right)^{2c}} \right] \quad (18)$$

where $\mathcal{D} = e^{1/(2g_{\perp})}$, $A = \frac{g_{\perp}}{2} + \frac{cg_{\perp}}{c+|g_z|}$, $B = AV^c$ with $c = \sqrt{g_z^2 - g_{\perp}^2}$. Here, we have neglected the subleading terms in Eq. 17 and Eq. 18 which depend logarithmically on V/D_0 .

We first look at the behavior of $M(h/V)$ at the KT transition. At a general level one might expect the nonequilibrium magnetization $M(h/V)$ at $T = 0$ in the de-localized phase behave in a similar way as the equilibrium thermal magnetization $M(h/T) = \tanh \frac{h}{2T}$ with T being replaced by V , leading to linear behavior in h/T at high temperatures. In equilibrium and at finite temperatures, it has been shown that the magnetization of a closely related model—a resonance-level with Ohmic dissipation—exhibits linear behavior in h/T at the KT transition. It is clear from Eq. 15 that the magnetization $M(h/V)$ in the equilibrium form based on the "flat approximation" ($g_{\perp}(\omega) \approx g_{\perp}(\omega = 0)$) always predicts a linear behavior in h/V . At the KT transition, we find the nonequilibrium magnetization $M(h/V)$ for $h \approx V$ also shows linear behavior, $M \approx h/V$. This can be understood from Eq. 13 as at the KT transition $g_{\perp}(0)/g_{\perp}(V/2) \approx 1$ for $V \approx h \ll D_0$. The Curie-law (linear) behavior in $M(h/V)$ here is reminiscent of the equilibrium thermal magnetization of a free spin in the high temperature regime. However, at the large bias voltages, $V \gg h$, we find a logarithmic correction to this linear behavior in M at the KT transition due to the nonequilibrium effect:

$$M \approx \frac{h}{V} \frac{1}{\left(1 - \frac{\pi}{4}\right) + \frac{\pi}{16} \left(\frac{\ln \frac{D_0^2}{hV}}{\ln \frac{D_0}{V}}\right)^2}. \quad (19)$$

This logarithmic suppression can be understood from Eq. 15 as in this case $g_{\perp}(\omega = 0)$ ($g_{\perp}(\omega = V/2)$) becomes peak (dip) and the ratio satisfies $g_{\perp}(V/2)/g_{\perp}(0) < 1$.

We now discuss $M(h/V)$ in the localized phase. First, in the limit of small bias, $V \approx h \ll D_0$, as the system gets deeper in the localized phase, $M(h/V)$ approaches to fully polarization $M = 1$ more rapidly than that at the KT transition. This is expected as the system gets deeper in the localized phase, the spin is more easily polarized upon applying a magnetic field. This behavior can also be explained from Eq. 13 as in the localized phase the ratio $g_{\perp}(0)/g_{\perp}(V/2) < 1$, and it only gets smaller as the system gets deeper in the localized phase. In fact, the same qualitative behavior is seen in a closely related Bose-Fermi Kondo model[3] which shows the KT transition between the Kondo and local moment ground states. In the large bias limit $V \gg h$, however, M deviates from the linear behavior due to nonequilibrium effects. The correction of M to linear behavior is dominated by the ratio $g_{\perp}(0)/g_{\perp}(V/2)$ via Eq. 15 where $g_{\perp}(\omega)$ shows deeper dips at $\omega = \pm V/2$, making $g_{\perp}(0)/g_{\perp}(V/2)$ to rapidly increase with decreasing h/V (see Fig. 7). This gives

rise to a further suppression of M at large bias voltages compared to that at the KT transition (see Fig. 6).

Note that from Fig. 5 and Fig. 6, as the system goes deeper into the localized phase (or with decrease in $g_{\perp} + g_z < 0$), we find M for a fixed $h \ll D_0$ increases for a fixed small bias voltage ($0.4 < h/V < 1$); while it decreases for a fixed large bias voltage ($h/V \ll 1$). This is in perfect agreement with the crossover behavior for M shown in Fig. 4.

Notice that the linear behavior of $M(h/V) \approx h/V$ is expected in purely asymmetric $g_{LR} > 0 = g_{LL/RR}$ but isotropic ($g_{LL/RR/LR,\perp} = g_{LL/RR/LR,z}$) Kondo model[12]. In a symmetric Kondo model with $g = g_{LL} = g_{RR} = g_{LR}$, the nonequilibrium magnetization $M(h/V)$ acquires an additional positive logarithmic corrections $M \approx (2h/V)(1 + 2g \ln |V/h|)$ [12]. In the present case, however, the deviation from the linear behavior of $M(h/V)$ in the large bias limit has a different origin. It comes from the fact that our effective Kondo model is not only asymmetric ($g_{LL/RR} = 0 < g_{LR}$) but also highly anisotropic ($g_{LR,z} \leq -|g_{LR,\perp}|$) at the KT transition and in the localized phase. Different corrections to the linear behavior are expected.

Susceptibility χ

The nonequilibrium charge susceptibility $\chi(V) \equiv \frac{\partial n_d}{\partial h}$ in the dissipative resonance-level is obtained from the spin susceptibility $\chi = \frac{\partial M}{\partial h}$ in the effective Kondo model by the mapping mentioned above. The susceptibility χ of a Kondo dot in equilibrium at finite temperatures is given by the Curie's law $\chi = \frac{1}{2T}$. However, in our highly asymmetric and anisotropic Kondo model, we find the nonequilibrium susceptibility deviates significantly from the Curie law. As shown in Fig.8, at the KT transition, as bias voltage is increased, $\chi(V)$ first shows $1/V$ Curie-law behavior, followed by an increase and a peak around $h/V = 0.1$. In the large bias limit, $\chi(V)$ gets a logarithmic suppression (see Eq. 15):

$$\chi \approx \frac{1}{V} \frac{1}{\left(1 - \frac{\pi}{4}\right) + \frac{\pi}{16} \left(\frac{\ln \frac{D_0^2}{hV}}{\ln \frac{D_0}{V}}\right)^2} \quad (20)$$

Note that the rapid increase in $\chi(h/V)$ at the KT transition with decreasing h/V for $0.1 < h/V < 0.5$ is reminiscent of the spin susceptibility of a nonequilibrium Kondo dot in a magnetic field where $\chi(h/V)$ acquires a logarithmic increase at large bias voltages[12]. On the other hand, the logarithmic decrease in $\chi(h/V)$ here at large bias is a direct consequence of the dip structure in $g_{\perp}(\omega)$ at the KT transition (see Eq. 16 and Fig. 9).

As the system gets deeper in the localized phase, $\chi(h/V)$ gets a more pronounced peak at $h \approx 0.7V$. As bias is further increased, $\chi(h/V)$ shows a similar trend

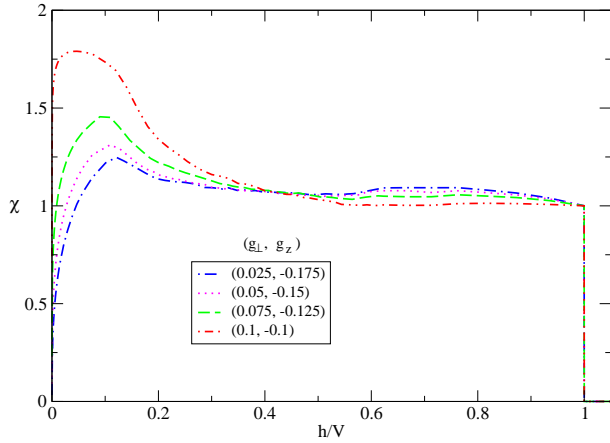


FIG. 8: (Color online) $\chi(h/V)$ versus h/V at the KT transition and in the localized phase. Here, the bare Kondo couplings $g_{\perp,z}$ are in units of D_0 , and $h = 10^{-9}D_0$ with $D_0 = 1$.

as that at the KT transition—a peak around $h/V = 0.1$ but smaller magnitudes (see Fig. 8). At large bias voltages, $V \gg h$, χ gets a more severe power-law suppression compared to the slower logarithmic decrease at the KT transition (see Fig. 9 and Eq. 17 and Eq. 18):

$$\chi \approx \frac{1}{V} \frac{1}{(1 - \frac{\pi}{4}) + \frac{\pi}{4} \frac{g_{\perp,loc}^2(0)}{g_{\perp,loc}^2(V/2)}} \quad (21)$$

with $g_{\perp,loc}(0), g_{\perp,loc}(V/2)$ given by Eq. 17 and Eq. 18. This comes as a result of further decrease in Kondo coupling $g_{\perp}(\omega)$ at $\omega = \pm V/2$ in the localized phase under RG.

We may compare the behavior in $\chi(V)$ in our model at large bias voltages with that in different limit of the same model or with different models. In the equilibrium limit $V \rightarrow 0$ within our model where $g_{\perp,z}(\omega)$ can be considered as flat functions over $-\frac{V+h}{2} < \omega < \frac{V+h}{2}$, $g_{\perp}(\omega = 0)/g_{\perp}(\omega = V/2) \approx 1$, a perfect Curie law behavior is expected for $\chi(V)$. However, for isotropic Kondo model ($g_{LL} = g_{RR} = g_{LR}$) for a simple quantum dot in Kondo regime and at large bias voltages, $\chi(V)$ shows Curie law with positive logarithmic correction, $\chi \approx \frac{1}{V} (1 + \frac{1}{\ln \frac{V}{T_k}})$ with T_k being Kondo temperature for a single quantum dot. In our dissipative resonance-level model, the suppression in $\chi(h/V)$ at large bias voltages at the KT transition and in the localized phase comes from the dips at $g_{\perp}(\omega = \pm V/2)$.

Conclusions

In conclusion, we have investigated the nonequilibrium occupation and charge susceptibility of a dissipative resonance-level with energy h . For $h = 0$, the system exhibits the Kosterlitz-Thouless type quantum transition between a de-localized phase at small dissipation

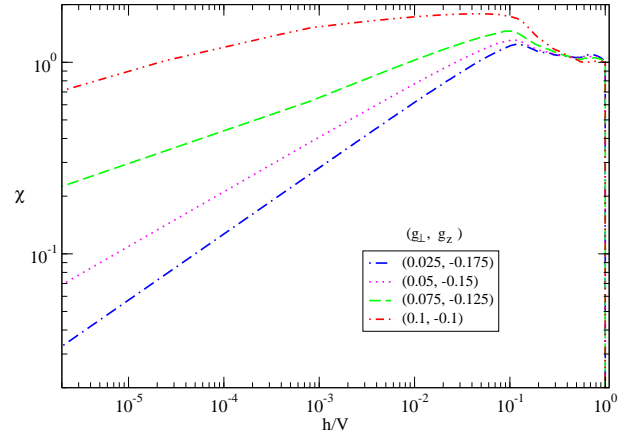


FIG. 9: (Color online) $\chi(h/V)$ versus h/V at the KT transition and in the localized phase. Here, the bare Kondo couplings $g_{\perp,z}$ are in units of D_0 , and $h = 10^{-9}D_0$ with $D_0 = 1$.

strength and a localized phase with large dissipation. We first mapped our problem onto an effective nonequilibrium anisotropic Kondo model in the presence of a magnetic field h . The occupation number and charge susceptibility correspond to magnetization M and susceptibility χ of the pseudospin in the effective Kondo model, respectively. By nonequilibrium RG approach, we solved for the frequency-dependent effective Kondo couplings and calculated magnetization $M(h/V)$ and $\chi(h/V)$ at finite bias voltages. We demonstrate the smearing of the KT transition in the nonequilibrium magnetization M at a fixed h as a function of the effective anisotropic Kondo couplings for both small bias and large bias voltages as it exhibits a smooth crossover at the KT transition, in contrast to a perfect jump in M at the transition in equilibrium. For small bias V and effective field h and $h \approx V$, we find the magnetization $M(h/V)$ at the KT transition shows linear behavior in h/V ; while in the localized phase M increases more rapidly with V approaching to h from above, consistent with the behaviors of the equilibrium magnetization in the localized phase at finite temperatures. In the large bias limit $V \gg h$, however, we find corrections to equilibrium Curie-law behavior in M due to nonequilibrium effects. At the KT transition, the corrections are logarithmic; in V/D_0 ; while in the localized phase they are power-law in V/D_0 . Our results have direct relevance for the transport measurements in nanostructures, and should stimulate further experiments.

We are grateful for the helpful discussions with P. Wölfle. This work is supported by the NSC grant No.98-2918-I-009-06, No.98-2112-M-009-010-MY3, the MOE-ATU program, the NCTS of Taiwan, R.O.C. (C.H.C.).

-
- [1] S. Sachdev, *Quantum Phase Transitions*, Cambridge University Press (2000).
- [2] S. L. Sondhi, S. M. Girvin, J. P. Carini, and D. Shahar, *Rev. Mod. Phys.* **69**, 315 (1987).
- [3] K. Le Hur, *Phys. Rev. Lett.* **92**, 196804 (2004); M.-R. Li, K. Le Hur, and W. Hofstetter, *Phys. Rev. Lett.* **95**, 086406 (2005).
- [4] K. Le Hur and M.-R. Li, *Phys. Rev. B* **72**, 073305 (2005).
- [5] P. Cedraschi and M. Büttiker, *Annals of Physics (NY)* **289**, 1 (2001).
- [6] A. Furusaki and K. A. Matveev, *Phys. Rev. Lett.* **88**, 226404 (2002).
- [7] L. Borda, G. Zarand, and D. Goldhaber-Gordon, *cond-mat/0602019*.
- [8] G. Zarand *et al.*, *Phys. Rev. Lett.* **97**, 166802 (2006).
- [9] G. Refael, E. Demler, Y. Oreg, and D. S. Fisher, *Phys. Rev. B* **75**, 014522 (2007).
- [10] J. Gilmore and R. McKenzie, *J. Phys. C* **11**, 2965 (1999).
- [11] C.H. Chung, K. Le Hur, M. Vojta and P. Wölfle, *Phys. Rev. Lett* **102**, 216803 (2009).
- [12] A. Rosch *et al.*, *Phys. Rev. Lett.* **90**, 076804 (2003); A. Rosch, J. Paaske, J. Kroha, P. Wölfle, *J. Phys. Soc. Jpn.* **74**, 118 (2005).